Process optimization and the relationship between the reaction degree and the antioxidant activity of Maillard reaction products of chicken liver protein hydrolysates

G. Y. Xiong,[*] X. Chen,[*,†] X. X. Zhang,[†] Y. Miao,[‡] Y. Zou,[†,1] D. Y. Wang,[†,1] and W. M. Xu[†]

[*]*Anhui Engineering Laboratory for Agro-products Processing, Anhui Agricultural University, Hefei, 230036, PR China;* [†]*Institute of Agricultural Products Processing, Jiangsu Academy of Agricultural Sciences, Nanjing 210014, PR China; and* [‡]*Jiangsu PICE Service Co., Ltd, Nanjing 210046, PR China*

ABSTRACT The aim of this study was to optimize the protein hydrolysates from chicken liver with xylose under Maillard reaction (**MR**) conditions using response surface methodology. The correlation between the browning degree, grafting degree, and the antioxidant activities of the Maillard reaction products (**MRPs**) was investigated. The optimal reaction conditions were achieved with a reaction temperature of 138.78°C, an initial pH of 7.99, and a reaction time of 93.14 min. The grafting degree (41.98%) and browning degree (2.582) of chicken liver protein hydrolysate MRPs (**CLPHM**) were notably higher ($P < 0.05$) than those of protein MRPs (**CLPM**) and were significantly lower ($P < 0.05$) than those of sonicated hydrolysate MRPs (**SCLPHM**). The reducing power, 2,2-diphenyl-1-picrylhydrazyl (DPPH) radical scavenging and hydroxyl radical scavenging of CLPM, CLPHM, and SCLPHM were significantly higher ($P < 0.01$) than those of the protein or hydrolysate substrates. The grafting degree and browning degree of CLPM, CLPHM, and SCLPHM had positive correlations with DPPH and hydroxyl radical scavenging activity. Hence, this study could enhance the added value of chicken liver by exhibiting the enhancements from ultrasound pretreatment and the MR. MRPs could have an effective and potential application in the food industry.

Key words: chicken liver, hydrolysates, Maillard reaction, correlation, antioxidant activity

2020 Poultry Science 99:3733–3741
https://doi.org/10.1016/j.psj.2020.03.027

INTRODUCTION

Chicken liver is a byproduct in the poultry industry with a large yield and low utilization rate and with a global production of more than 3 million tons per year (FAO, 2018). Especially in China, approximately half a million tons of chicken liver are obtained per year, accounting for 16.67% of the world's production. Chicken liver, a low-value but high-protein organ, is usually discarded as industrial waste, despite its edibility, during processing (Xiong et al., 2017). There are many reports with regard to extracting functional ingredients from chicken liver and improving its functional properties, such as antioxidant and antibacterial activities (Sun et al., 2010; Chakka et al., 2015), using enzymatic hydrolysis. In recent years, enzymatic hydrolysis has been an effective way to use byproducts to produce bioactive peptides, and it has gradually become a readily applied method in research (Jiang et al., 2019). Furthermore, ultrasound-assisted treatment is an effective and new technique to extract proteins and improve their functional characteristics. Zhang et al. (2015) reported that ultrasound-assisted heating could improve the solubility of chitosan-fructose and its antioxidant activities. Compared to that of synthetic antioxidants, the bioactive peptide from protein hydrolysis also manifested lower antioxidant activity (Nooshkam et al., 2016). However, Maillard reaction (**MR**) modification is an effective method to solve these problems (Nie et al., 2017; Han et al., 2018).

The MR is a nonenzymatic browning reaction involving amino groups (amino acids, peptides, and proteins) and carbonyls (reducing sugars), which occurs during heating (Habinshuti et al., 2019). The reaction forms Amadori substances and irreversible advanced glycation end-products via rearrangement through subsequent reactions (Yang et al., 2015; Habinshuti et al., 2019). The MR could improve the color of food as well as enhance its aroma with Maillard reaction products (**MRPs**)

Received October 9, 2019.
Accepted March 20, 2020.

[1]Corresponding authors: zouye@jaas.ac.cn (YZ); wdy0373@aliyun.com (DYW)

compared with the color and aroma of reaction substances (Zeng et al., 2012). However, recent studies demonstrated that some MRPs have functional activities, such as antioxidant activity (Favre et al., 2018) or antibrowning activities (Yang et al., 2015). Many factors can influence the properties and type of MRPs, such as substrate concentration, reaction time, initial pH, and reaction temperature (Favre et al., 2018). However, few studies have focused on the interaction between different degrees of protein hydrolysate, especially byproduct protein hydrolysate. Owing to the development and improvement in statistical and mathematical techniques, response surface methodology (RSM) can be used to evaluate more experimental conditions for the optimization of multiple factors and their interaction with respect to response variables (Zeng et al., 2018).

In this study, we used RSM to obtain optimum reaction conditions for the MR with chicken liver protein (**CLP**) that had undergone limited hydrolysis with xylose and compared the antioxidant activities between its MRPs and the substrates with or without ultrasound treatment (CLP, sonicated chicken liver protein hydrolysate [**SCLPH**], and chicken liver protein hydrolysate [**CLPH**]). Furthermore, this study confirmed the correlation of the antioxidant activities of these MRPs with their grafting and browning degrees.

MATERIALS AND METHODS

Chemicals and Materials

Chicken liver was obtained from a commercial slaughterhouse (Jiangsu Lihua Co., Ltd, Changzhou, China), which was placed in crushed ice packaged in vacuum bags and then quickly transported to the laboratory at −18°C for storage. D-xylose, sucrose, D-galactose, D-fructose, glucose, and maltose were purchased from Sinopharm Chemical Reagent Co., Ltd. (Shanghai, China). Pancreatin, 2,2-diphenyl-1-picrylhydrazyl (DPPH), ferrozine mono-sodium salt, o-phthaldialdehyde (**OPA**), and L-carnosine were supplied by Shanghai Yuanye Biotechnology Co., Ltd. (Songjiang District, Shanghai, China). All other reagents used were of analytical grade.

Preparation of CLPH

CLPH was prepared as reported by Liu et al. (2010), with slight modifications. After removing fat and fascia, chicken livers were minced and heated at 100°C for 20 min to inactivate endogenous enzymes. One hundred grams of sample was treated for 12 h with 10% isopropanol at 1:10 (w/v). The solution was centrifuged at 10,000 rpm at 4°C to remove the supernatant. The defatted chicken liver was mixed with pH 8.0 NaOH solution (add 0.5 mol NaOH solution to deionized water until pH reach 8.0) at 50°C at a ratio of 1:6 (w/v). Protein hydrolysis was conducted using trypsin (4,000 U/g). The hydrolysates were heated at 100°C for 20 min to inactivate enzymes. Subsequently, the solution was centrifuged at 5,000 rpm for 15 min at 4°C. The hydrolysates of desired degrees of hydrolysis (**DHs**) (DH of 5, 10, 15, 20, and 25%) were lyophilized, and the others were used for further MRP preparation. CLP was the control group. The calculation of the DH was based on the following formula (Zou et al., 2016):

$$DH(\%) = \frac{h}{h_{tot}} = \frac{N_b \times B}{\alpha \times M_p \times h_{hot}}$$

where N_b is the concentration of NaOH (mol/L), B is the volume of NaOH consumed (mL), M_p is the mass of protein to be hydrolyzed (g), h_{tot} is the total number of peptide bonds in the protein substrate, which is 7.6 mmol/g for porcine cerebral protein, and α is the average degree of dissociation of the α-NH_2 groups.

Preparation of MRPs

MRPs were prepared in accordance with the method reported by Habinshuti et al. (2019), with minor modifications. CLPH (DH of 5-25%) and reducing sugar (D-xylose, sucrose, D-galactose, D-fructose, glucose, and maltose) were mixed at the mass ratio of 1:1. The solutions were transferred and sealed into 35-mL screw-sealed glass tubes. Then the tubes were heated in a thermostatic oil bath with magnetic stirring. Subsequently, the reaction was stopped using an ice bath, and the solution was centrifuged with a high-speed refrigerated centrifuge at 10,000 rpm for 10 min. The supernatant was directly used for determining browning intensity and UV-absorbance, while the rest of the sample was freeze-dried and stored at −20°C for further use.

A solution of 5% (w/v) CLPH was pretreated by ultrasound with a 2.0-cm flat tip probe operating in a sequence of 2 s of sonication and 3 s of rest, which obtained the solution of SCLPH (Zou et al., 2019a,b). A probe ultrasonic reactor (SCIENTZ-IID; Ningbo Xinzhi ultrasonic technology co., LTD, Zhejiang, China) working with a power of 200 W was used for 12 min (Chen et al., 2019). Then, the mixture of hydrolysates and xylose was adjusted to a pH of 7.99 with NaOH (0.5 mol) and allowed to react at the optimal condition, which obtained CLPHM and SCLPHM, respectively. CLP was the control group.

Experimental Design

According to the previous experiment, a DH of 20% for CLPH was optimum for the MR. The reaction conditions were obtained in a previous single experiment (no data provided), including the optimization of temperature (90–140°C), initial pH (6.0–8.5), and reaction time (50–100 min). The MR conditions were optimized through a Box-Behnken design (**BBD**). RSM with a BBD was used to predict the browning degree of Maillard reaction products (**CLPHM**) of CLPH via heating temperature (X_1), initial pH (X_2), and time (X_3). BBD with independent variables applied to a total 17 experiments was found to be sufficient for calculating the coefficients of the model for one variable. Each variable

was investigated at 3 levels: −1, 0, and 1, as shown in Table 1. The Design-Expert V8.0.6 software (Stat-Ease Inc., Minneapolis, MN) was used to generate the experimental design.

Determination of Browning and UV-absorbance

Browning intensities and UV-absorbance of these MRPs were determined according to the methods published by Jiang et al. (2013), with slight modifications. The degree of browning (**DB**) and UV-absorbance of these MRPs were assessed by absorbance readings at 420 and 294 nm against water using a UV-visible spectrophotometer (UV-2401PC; Shimadzu Co., Ltd., Kyoto, Japan). Samples were diluted 4-fold and 16-fold with deionized water for browning intensity and UV-absorbance analysis, respectively.

Degree of Grafting Assay

The grafting degree of MRPs was quantified by the OPA method illustrated by Jiang et al. (2013), with slight modifications. The sample was diluted to a protein concentration of 1 mg/mL. Two hundred microliters of sample was mixed with 4 mL of OPA reagent. The sample was blended and incubated in darkness at 37°C for 30 min, and the absorbance was recorded at 340 nm against the OPA reagent. A bank sample was run in the same manner, except that deionized water was used instead of the samples. The grafting degree was calculated according to the following formula:

$$\mathrm{DG}(\%) = \frac{\mathrm{A_0} - \mathrm{A_t}}{\mathrm{A_0}} \times 100\% \quad (2)$$

where A_0 is the absorbance of the blank and A_t is the absorbance of the samples.

Determination of Antioxidant Activity

Determination of reducing power

Reducing power of the samples was determined according to the method illustrated by Liu et al. (2010), with slight modifications. Half a milliliter of 0.2 mol sodium phosphate buffer (pH 6.6) and 0.5 mL of 1.0% potassium ferricyanide were mixed with 0.5 mL of MRP solutions (0.01, 0.05, 0.1, 0.5, 1, and 2 mg/mL) of different concentrations. The mixtures were incubated in a temperature-controlled water bath at 50°C for 20 min. The samples were cooled in an ice bath, and then 0.5 mL of 10% trichloroacetic acid was added. The mixture was then centrifuged, and the supernatant obtained (1 mL) was treated with 1 mL of distilled water and 1 mL of 0.1% $FeCl_3$. The absorbance of the reaction mixture was measured at 700 nm. An increase in absorbance was regarded as the enhancement of reducing power.

DPPH Free Radical Scavenging Activity Assays

The DPPH free radical scavenging activity was determined using the method explained by Lin et al. (2019), with slight modifications. One hundred microliters (μL) of DPPH solution (0.1 mmol in absolute ethanol) was added to 100 μL of MRP solutions of various concentrations (0.01, 0.05, 0.1, 0.5, 1, and 2 mg/mL). The mixed solution was shaken well and incubated in the dark for 1.5 h at 37°C. Afterward, the absorbance of the solution was recorded at 517 nm. Ascorbic acid was used as the positive control. The DPPH radical scavenging rate was calculated by using Eq. (3):

$$DPPH\ scavenging\ rate\ (\%) = \left(1 - \frac{Abs_{sample} - A_{blank}}{Abs_{control}}\right) \times 100 \quad (3)$$

Table 1. The design and results of the response surface analysis test.

	Factors			
No.	X_1 (heating temperature)	X_2 (initial pH)	X_3 (time)	Degree of browning (DB)
1	120	8.0	80	1.456
2	130	7.5	100	1.962
3	130	8.0	90	2.149
4	120	8.5	90	1.415
5	130	7.5	80	1.788
6	130	8.0	90	2.157
7	130	8.0	90	2.164
8	120	7.5	90	1.576
9	140	8.0	80	1.78
10	130	8.0	90	2.16
11	140	8.0	100	1.98
12	120	8.5	100	1.86
13	130	8.0	90	2.157
14	140	8.5	90	1.857
15	120	8.0	100	1.583
16	130	8.5	80	1.753
17	140	7.5	90	1.86

The DPPH solution added to the MRP or the ascorbic acid solution was used as the sample; ethanol added to the solution of MRPs was used as the blank, and ethanol added to the DPPH solution was used as the control.

Hydroxyl Radical Scavenging Activity Assay

The hydroxyl radical scavenging activity was measured according to the method of Jiang et al. (2019), with slight modifications. Samples of CLPH and its MRPs with different concentrations (0.01, 0.05, 0.1, 0.5, 1, and 2 mg/mL) were prepared in distilled water. Then, 50 μL of each sample was mixed with 50-μL salicylic acid (10 mmol/L, in ethanol), 50-μL ferrous sulfate (1.0 mmol), and 100-μL H_2O_2 (0.5 mol). The mixture was incubated at room temperature for 10 min. The absorbance of the reaction was noted at 510 nm. Hydroxyl radical scavenging activity was calculated using the following formula:

$$\textit{Hydroxyl radical scavenging activity}(\%) = \left(1 - \frac{A_1 - A_2}{A_3}\right) \times 100 \quad (4)$$

where A_1 is the absorbance of the sample, A_2 is the absorbance of the control (Ferrous sulfate was replaced by distilled water.), and A_3 is the absorbance of the blank (The sample was replaced by distilled water.).

Statistical Analysis

All experiments were carried out in triplicate. Means and standard deviations of the data were calculated for each treatment. ANOVA was carried out to determine significant differences ($P < 0.05$). The curve fitting and correlation analysis were performed using Origin 8.5 and IBM SPSS Statistics 23.0 (IBM, Armonk, NY), respectively. The least significant difference test and Pearson's test were performed for multiple comparisons and correlation analysis, respectively. All statistical analyses were carried out at a 95% confidence level.

RESULTS AND DISCUSSION

DH and Reducing Sugar

The DH of the hydrolysates contributed to the developed molecules. The larger the DH of the hydrolysates, the smaller the molecular weight of the hydrolysate. Figure 1A shows the absorbance of different MRPs at 420 nm and 294 nm. In different DH, the absorbance of hydrolysates at 420 nm and 294 nm were not significant. The absorbance at 420 nm and 294 nm of hydrolysates was ∼0.162 and ∼0.304, respectively, which was both lower than that of hydrolysates MRPs (Data were not given in Figure 1A). Moreover, the absorbance at 420 nm and 294 nm of the hydrolysates MRPs were both higher than those of the control group (A_{420nm} was 0.223 and A_{294nm} was 0.351). The absorbance increased

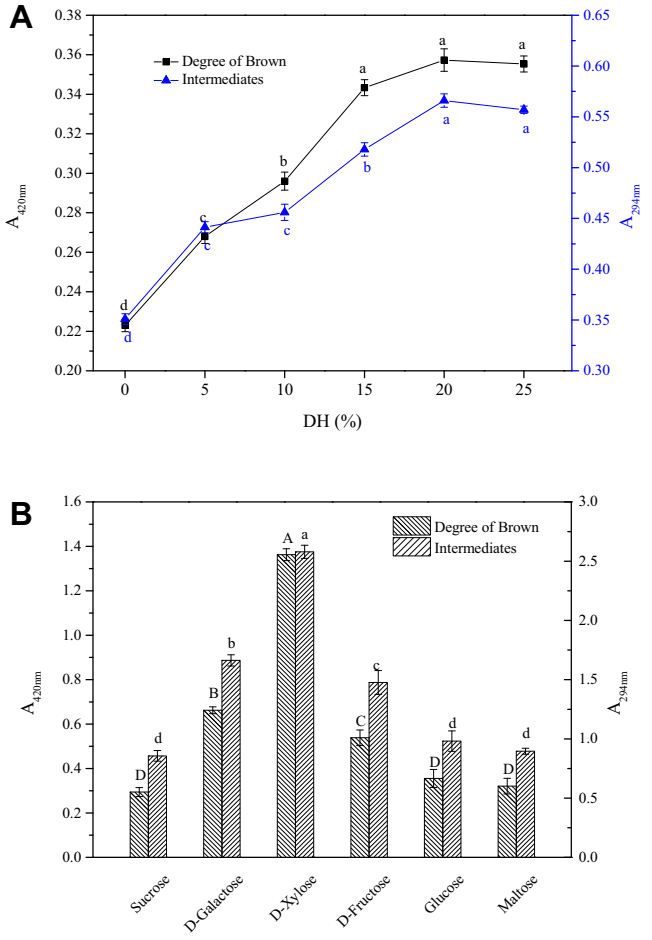

Figure 1. Degree of browning and intermediates of Maillard reaction products. (A) Different degrees of hydrolysis; (B) Different reducing sugars. The results are represented as the mean value ± SD of each treatment (n = 4). Means without a common letter significantly differ ($P < 0.05$).

with the increase in DH. The DB and intermediates of MRPs were the highest when DH was 20%. The spatial structure of the protein was damaged, causing the thermal treatment and cavitation effect. The peptide generated a small molecular peptide chain or free amino acids through trypsin. Lower molecular weight peptides easily combined under controlled Maillard-induced glycation and had higher absorbance of browning and intermediate compounds (Walter et al., 2016; Nie et al., 2017). In addition, the absorbance of the hydrolysate with a DH at 25% slightly decreased from that with a DH of 20%. This may be relevant that the hydrolysates accelerated the progress of the reaction, causing the intermediates and chromophore substances to undergo aggregation and sedimentation during the reaction (Malaypally et al., 2015). Therefore, a DH of 20% of protein hydrolysates was selected for further studies in the following experiments.

Figure 1B shows the absorbance of MRPs obtained from different reducing sugars at 420 nm and 294 nm. The absorbance was the highest in D-xylose. This may be related to the fact that D-xylose is a 5-carbon sugar with a small molecular weight that easily reacts with proteins or protein hydrolysates (Cai et al., 2016;

Zou et al., 2019a,b). The MR progressed quickly between D-xylose and porcine bone protein hydrolysate.

Fitting the Model

Table 1 shows the values of independent variables (heating temperature, initial pH, and reaction time) used in RSM for optimizing the DB of CLPHM. Experiment #7 (a reaction temperature of 130°C, an initial pH of 8.0, and a reaction time of 90 min) provided the highest DB (2.164). Experiment #1 (a reaction temperature of 120°C, an initial pH of 8.0, and a reaction time 80 min) obtained the lowest DB.

The ANOVA is presented in Table 2. The experimental values of all the response data can be fitted using a quadratic polynomial model (P value < 0.0001). The F-value of 1,633.94 for the DB of the MRPs suggested that the significance of the model was higher than the 95% confidence level. In Table 2, the "Lack of Fit F-value" of 3.95 implied the Lack of Fit F-value was not significant relative to the pure error. There is a 10.90% chance that a "Lack of Fit F-value" this large could occur because of noise. Nonsignificant lack of fit is good, and we think the model would fit. "Adeq Precision" measures the signal to noise ratio. A ratio greater than 4 is desirable. In this study, the ratio of 116.270 indicated an adequate signal, which indicate the good reproducibility of the experimental data.

The effects of reaction conditions X_1 (reaction temperature), X_2 (initial pH), and X_3 (reaction time) were carefully analyzed for each response factor (Table 1). The F-value and P-value determined the significance of each coefficient, considering that a higher F-value with a lower P-value always led to a more significant correspondence between various independent variables (Favre et al., 2018).

Response Surface Analysis of Browning Intensity

Table 2 shows the results of applying the quadratic polynomial equation for the browning intensity and reaction parameters (heating temperature, initial pH, and reaction time). The acceptable regression value ($R^2 = 0.9989$) proved the reliability of the model. We generated the following regression equation at the coded level to analyze the effect of each independent variable on the browning intensity of the CLPHM.

$$Y(DB,\ Abs) = 2.16 + 0.18X_1 - 0.038X_2 + 00076X_3 + 0.039X_1X_2 + 0.018X_1X_3 - 0.017X_2X_3 - 0.31X_1^2 - 0.17X_2^2 - 0.15X_3^2$$

The analysis of the applied model showed that all independent variables were significant parameters on the combined factor reaction condition of the browning intensity of the CLPHM. The combination of variables X_1X_2, X_1X_3, and X_2X_3 showed a synergistic effect.

Figure 2 represents the mutual interaction between the browning intensity of CLPHM and the reaction variable parameters (reaction temperature, reaction time, and initial pH). Figure 2A and B shows that the browning intensity of CLPHM increased with increasing initial pH when the reaction temperature remained constant at 138.78°C. The contour line was elliptical, which indicated that the reaction temperature and initial pH had a significant effect on the MR. Figure 2C and D shows the relationship between reaction temperature and reaction time for the browning intensity of CLPHM. The browning intensity of CLPHM increased with prolonged reaction time when the reaction temperature was constant at 138.78°C. The contour plot indicated that the mutual interaction between reaction temperature and reaction time was a significant parameter for the browning intensity of the MR. The browning intensity increased as the reaction time increased when the initial pH was held constant at pH 7.99 (Figure 2E). The synergistic effect of reaction time and initial pH had a significant effect on the browning degree of the MRPs, as shown in Figure 2F. These results confirmed the validity of the applied model for predicting the DB. According to these results, the highest DB of the MRPs was obtained for the reaction condition parameters (a reaction temperature of 138.78°C, an initial pH of 7.99, and a reaction time of 93.14 min) previously reported in Table 1.

Degree of Grafting

Grafting degree is an indicator of the degree of reaction of the MR. The grafting degree of CLPHM was significantly different from that of CLPM, as shown in Figure 3 ($P < 0.05$). The browning degree of CLPHM was consistent with the grafting degree, which was significantly higher than that of CLPM ($P < 0.05$). The spatial structure of the protein was opened, and the peptide bonds were broken via enzymatic hydrolysis. In the reaction system, the increase in free amino acid content enhanced the probability of contact with xylose, which promoted the occurrence

Table 2. ANOVA for the fitted quadratic polynomial model for optimization of reaction parameters.

Source	Sum of squares	Df	Mean square	F value	P value	Significant
Model	1.01	9	0.11	1,633.94	<0.0001	*
Residual	0.0004799	7	0.00006856			
Lack of fit	0.0003587	3	0.0001196	3.95	0.1090	
Pure error	0.0001212	4	0.00003030			
Toal	1.01	16				
			$R^2_{Adj} = 0.9989$	adeq precision = 116.27		

*Highly significant difference.

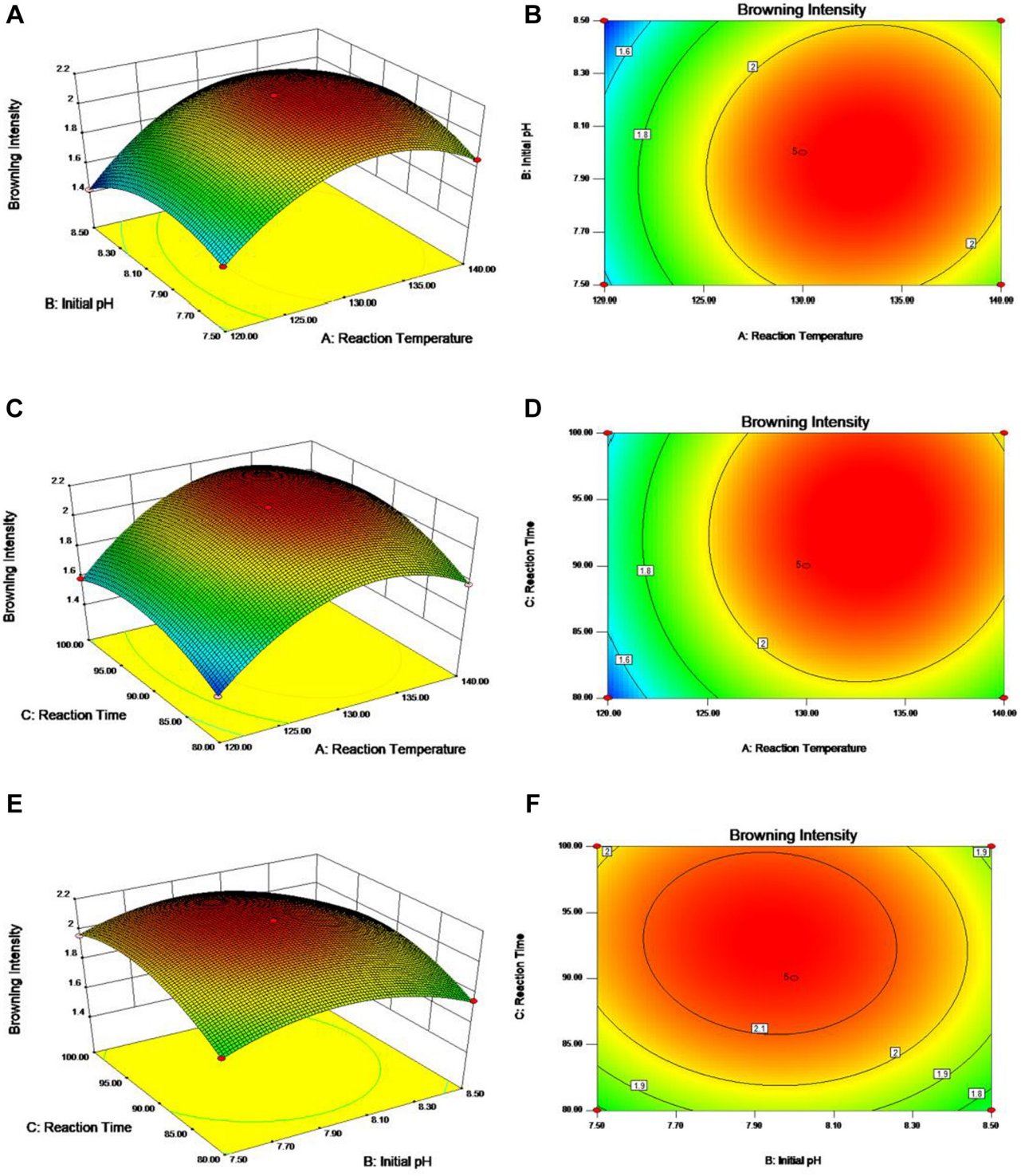

Figure 2. Response surfaces and contour plots of independent variables for the browning intensity (BI) of CLPHM showing the maximum for the variable combinations. BI as a function of (A, B) reaction temperature and initial pH using a constant reaction time of 93.14 min; (C, D) reaction temperature and reaction time using a constant initial pH of 7.99; (E, F) initial pH and reaction time using a constant reaction temperature of 138.78°C.

of the MR. Fu et al. (2016) reported that the degree of the MR increased with an increasing degree of enzymatic hydrolysis and reaction time. In addition, the grafting degree and browning degree of SCLPHM were significantly higher than those of CLPHM ($P < 0.05$). Ultrasound could alter the spatial structure of the protein and increase the bonds between the peptide and xylose. However, as the reaction progresses, the generated macromolecular substances undergo aggregation and sedimentation (Guan et al., 2010; Zhang et al., 2015).

Antioxidant Activity of MRPs

Reducing power Assay The reducing power is related to the concentration of the samples, as shown in

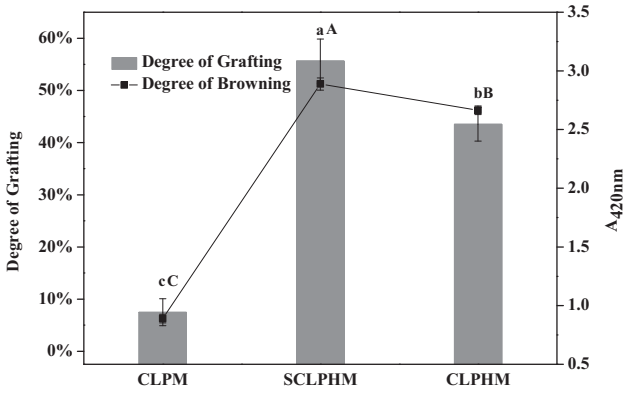

Figure 3. Effect of different treatments of chicken liver protein hydrolysates on the degree of grafting and browning of the MRPs. a, b, c: the mean ± SD (n = 3) of the degree of grafting with the same letter is not significantly different ($P < 0.05$). A, B, C: the mean ± SD (n = 3) of the degree of browning with the same letter is not significantly different ($P < 0.05$).

Figure 4A. The absorbance at 700 nm increases as the concentration increases, which indicated that the activity of reduction was enhanced. The absorbance of the MRPs was significantly higher than that of its substrate, such as CLP, SCLPH, and CLPH ($P < 0.05$). SCLPHM and CLPHM showed the highest reducing power at a concentration of 0.5 mg/mL. The reducing power of CLPH was notably higher than that of CLP and significantly lower than that of SCLPH ($P < 0.05$). Protein hydrolysis MRPs increased the free hydroxyl content and provided hydrogen atoms to break the radical chain, causing an increase in reducing power activity (Liu et al., 2010; Hwang et al., 2011). Macromolecular substances of CLP have less ability to provide hydrogen atoms. After hydrolysis, the molecular weight of CLPH decreased, providing more hydrogen atoms, which increases the reducing power of CLPH (Chakka et al., 2015). Ultrasound treatment promoted the brekage of intramolecular hydrogen bonds, leading to more hydroxyl groups being exposed and causing the stronger hydrogen donating ability (Zhang et al., 2015). Sun et al. (2014) reported that MRPs from whey protein peptides (WPP-MRPs) possessed strong antioxidant activity. Moreover, ultrasonic action enhanced molecular motion between the amino groups and the carbonyl groups, producing more antioxidants, such as pyrazine and Schiff bases. These results revealed that high-intensity ultrasound could improve the antioxidant properties of chitosan-fructose MRPs (Zhang et al., 2015).

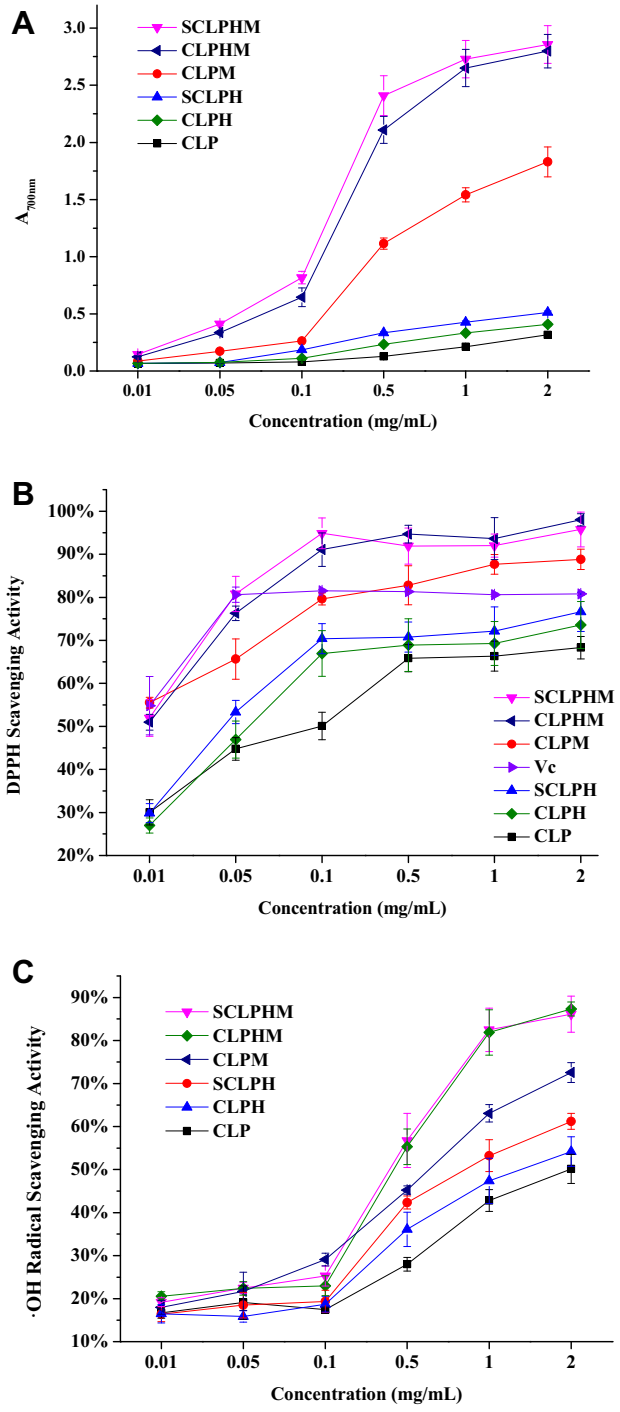

Figure 4. Antioxidant activity of different concentrations of CLPH and its hydrolysates before and after the Maillard reaction with xylose. Reducing power (A); DPPH radical scavenging activity (B); and hydroxyl radical scavenging activity (C).

DPPH Radical-Scavenging Activity Assay

The scavenging activity of CLP, SCLPH, CLPH, and their MRPs on the DPPH radical increased with the increase in their concentration, but no further changes were reflected when the concentration reached a certain extent. Before the MR, DPPH radical scavenging activity was observed in the order of decreasing activity of SCLPH > CLPH > CLP, and they were significantly lower than the activity of their MRPs, as shown in Figure 4B. Among SCLPHM, CLPHM, and CLPM, the DPPH radical scavenging activity was significantly higher than that of the ascorbic acid positive control when the concentration was more than 0.5 mg/mL. Sonication enhanced the DPPH radical scavenging capacity of the MRPs, and the results of the DPPH radical scavenging activity were similar to those of reducing power. In addition, the free radicals of the DPPH molecule can capture the hydrogen atoms of the antioxidant molecule. The molecule can then be stabilized and would not be able to propagate to chain reaction (Balakrishna et al., 2019;

Table 3. Correlation analysis between the grafting degree and the antioxidant activity of MRPs.

Experiment index	DG	DB	Reducing power	DPPH radical scavenging activity	Hydroxyl radical scavenging activity
DG	1	0.961**	0.161	0.771**	0.976**
DB		1	0.127	0.826**	0.975**
Reducing power			1	-0.001	0.134
DPPH radical scavenging activity				1	0.779**
Hydroxyl radical scavenging activity					1

*Significant difference at $P < 0.05$. **Significant difference at $P < 0.01$.
Abbreviations: DB, degree of browning; DG, degree of grafting; DPPH, 2,2-diphenyl-1-picrylhydrazyl; MRP, Maillard reaction product.

Habinshuti et al., 2019). These results were in accordance with those of Guan et al. (2010), who found that the DPPH radical scavenging ability of ultrasound-assisted MRPs of whey protein hydrolysate reached its maximum level and was significantly higher than that of the control. The DPPH radical scavenging activity of SCLPHM was similar to the grafting degree and browning degree. Jiang et al. (2013) noted that intermediate and brown compounds formed during the MR could function as hydrogen donors to form stable DPPH-H molecules.

Hydroxyl Radical Scavenging Activity Assay

Hydroxyl radicals are highly reactive oxygen species. The hydroxyl radical scavenging rate is an important indicator for evaluating free radical scavenging ability. Therefore, the scavenging activity against hydroxyl radicals is one of the most effective protections against various diseases caused by radical-induced oxidative stress (Alemán et al., 2011, Nie et al., 2017, Xiong et al., 2019). Figure 4C shows the hydroxyl radical scavenging activities of CLP, hydrolysates, and their MRPs. The hydroxyl radical scavenging activity of each sample had no significance when the concentration was below 0.1 mg/mL. CLP and its hydrolysates are poor scavengers of hydroxyl radicals than hoki frame peptides (Kim et al., 2007). This may be due to the difference in concentration and type of peptide. The activity of SCLPHM and CLPHM was higher than that of CLPM and the hydrolysates, consistent with the results of reducing power (Figure 4A). However, there was no significant difference between the hydroxyl radical scavenging ability of SCLPHM and CLPHM, which might be due to insufficient ultrasound time to cleave the protein structure or to aggregate proteins during ultrasound processing. The inhibition of MRPs by hydroxyl radicals might be relevant to their metal chelating ability and hydrogen peroxide scavenging activity (Nie et al., 2017). In addition, the improvement of the hydroxyl radical scavenging activity of MRPs may be attributed to the Amadori components, which contain chromogenic groups, deoxy-fructose, pyrrolidone, and reducing ketones (Shizuuchi, 2003).

Correlation Analysis

Table 3 shows the correlation among degree of grafting (DG) and DB and the antioxidant activity of the MRPs. According to the correlation analysis, DG showed a significantly positive correlation with DB ($r = 0.961$, $P < 0.01$), DPPH radical scavenging activity ($r = 0.771$, $P < 0.01$), and hydroxyl radical scavenging activity ($r = 0.976$, $P < 0.01$). Such significant correlations indicated that increased DG and DB were both favorable for the improvement in DPPH radical scavenging activity and hydroxyl radical scavenging activity. In addition, these results are in agreement with the findings of Wang et al. (2018) and Abakarov et al. (2010). Furthermore, the increase in DG and DB indicated that the reaction produced intermediates of MRPs. The DPPH radical scavenging activity and hydroxyl radical scavenging activity increased with increasing browning and grafting degrees.

CONCLUSIONS

According to the RSM, the study achieved the optimized reaction hydrolysis conditions of CLPH with xylose. In comparison with CLPM, the DG and browning of SCLPHM and CLPHM were enhanced significantly. Limited hydrolysis of liver protein greatly improved the process of MR and enhanced the antioxidant activity. In addition, the antioxidant activities of chicken liver MRPs had a positive correlation with the browning degree and grafting degree. Therefore, this study can increase the added value of chicken liver, and its MRPs could have an effective and potential application in the food industry.

ACKNOWLEDGEMENTS

This work was supported by the China Agriculture Research System (CARS-41), the Anhui Provincial Natural Science Foundation (1808085MC92), the Agricultural Science and Technology Independent Innovation Project of Jiangsu Province (CX (18)1006), and the Fundamental Research Funds for the Jiangsu Academy of Agricultural Sciences (ZX(18)1005).

Conflict of interest: The authors declare that they have no conflicts of interest regarding the contents of this article.

REFERENCES

Abakarov, A., A. Barahona, R. Simpson, and S. Almonacid. 2010. Improvement of functional properties of salmon processing protein-rich by-product through hydrolysis and Maillard reaction. J. Biotechnol. 150:309.

Alemán, A., B. Giménez, P. Montero, and M. C. Gómez-Guillén. 2011. Antioxidant activity of several marine skin gelatins. LWT - Food Sci. Technol. 44:407–413.

Balakrishna, M., J. Ma, Z. Geng, T. Liu, P. Li, D. Wang, M. Zhang, and W. Xu. 2020. Hydrolysis of oxidized phosphatidylcholines by crude enzymes from chicken, pork and beef muscles. Food Chem. 313:125956.

Cai, L., D. Li, Z. Dong, A. Cao, H. Lin, and J. Li. 2016. Change regularity of the characteristics of Maillard reaction products derived from xylose and Chinese shrimp waste hydrolysates. LWT - Food Sci. Technol. 65:908–916.

Chakka, A. K., M. Elias, R. Jini, P. Z. Sakhare, and N. Bhaskar. 2015. In-vitro antioxidant and antibacterial properties of fermentatively and enzymatically prepared chicken liver protein hydrolysates. J. Food Sci. Tech. 52:8059–8067.

Chen, W., X. Ma, W. Wang, R. Lv, M. Guo, T. Ding, X. Ye, S. Miao, and D. Liu. 2019. Preparation of modified whey protein isolate with gum acacia by ultrasound maillard reaction. Food Hydrocolloid 95:298–307.

FAO. 2018. FAOSTAT Domains. Food and Agriculture organization of the United Nations. Accessed May 2019. http://faostat3.fao.org/faostat-gateway/go/to/do-wnload/Q/QL/E.

Favre, L. C., C. Dos Santos, M. P. López-Fernández, M. F. Mazzobre, and M. del P. Buera. 2018. Optimization of β-cyclodextrin-based extraction of antioxidant and anti-browning activities from thyme leaves by response surface methodology. Food Chem. 265:86–95.

Fu, J. Y., W. D. Bai, Y. R. Liu, and Q. Wang. 2016. Improving the functional properties of chicken protein in maillard reaction by hydrolysis. Mod. Food Sci. Technol. 32:186–195.

Guan, Y. G., J. Wang, S. J. Yu, X. B. Xu, and S. M. Zhu. 2010. Effects of ultrasound intensities on a glycin-maltose model system - a means of promoting maillard reaction. Int. J. Food Sci. Technol. 45:758–764.

Habinshuti, I., X. Chen, J. Yu, O. Mukeshimana, E. Duhoranimana, E. Karangwa, B. Muhoza, M. Zhang, S. Xia, and X. Zhang. 2019. Antimicrobial, antioxidant and sensory properties of Maillard reaction products (MRPs) derived from sunflower, soybean and corn meal hydrolysates. LWT - Food Sci. Technol. 101:694–702.

Han, J. R., J. N. Yan, S. G. Sun, Y. Tang, W. H. Shang, A. T. Li, X. K. Guo, Y. N. Du, H. T. Wu, B. W. Zhu, and Y. L. Xiong. 2018. Characteristic antioxidant activity and comprehensive flavor compound profile of scallop (Chlamys farreri) mantle hydrolysates-ribose Maillard reaction products. Food Chem. 261:337–347.

Hwang, I. G., H. Y. Kim, K. S. Woo, J. Lee, and H. S. Jeong. 2011. Biological activities of Maillard reaction products (MRPs) in a sugar–amino acid model system. Food Chem. 126:221–227.

Jiang, W., Y. Liu, X. Yang, and S. Hu. 2019. Antioxidant and antibacterial activities of modified crab shell bioactive peptides by Maillard reaction. Int. J. Food Prop. 21:2730–2743.

Jiang, Z., L. Wang, W. Wu, and Y. Wang. 2013. Biological activities and physicochemical properties of Maillard reaction products in sugar-bovine casein peptide model systems. Food Chem. 141:3837–3845.

Kim, S. Y., J. Y. Je, and S. K. Kim. 2007. Purification and characterization of antioxidant peptide from hoki (Johnius belengerii) frame protein by gastrointestinal digestion. J. Nutr. Biochem. 18:31–38.

Lin, Q. Z., M. Li, L. Xiong, L. Qiu, X. Bian, C. Sun, and Q. Sun. 2019. Characterization and antioxidant activity of short linear glucan–lysine nanoparticles prepared by Maillard reaction. Food Hydrocolloid 92:86–93.

Liu, P., M. G. Huang, S. Q. Song, K. Hayat, X. M. Zhang, S. Q. Xia, and C. S. Jia. 2012. Sensory characteristics and antioxidant activities of maillard reaction products from soy protein hydrolysates with different molecular weight distribution. Food Bioproc. Technol 5:1775–1789.

Malaypally, S. P., A. M. Liceaga, K. H. Kim, M. Ferruzzi, F. S. Martin, and R. R. Goforth. 2015. Influence of molecular weight on intracellular antioxidant activity of invasive silver carp (Hypophthalmichthys molitrix) protein hydrolysates. J. Funct. Foods 18:1158–1166.

Nie, X. H., D. Xu, L. M. Zhao, and X. H. Meng. 2017. Antioxidant activities of chicken bone peptide fractions and their Maillard Reaction Products Effects of different molecular weight distribution. Int. J. Food Prop. 20:457–466.

Nooshkam, M., and A. Madadlou. 2016. Maillard conjugation of lactulose with potentially bioactive peptides. Food Chem. 192:831–836.

Shizuuchi, S., and F. Hayase. 2003. Antioxidative activity of the blue pigment formed in a D-xylose-glycine reaction system. Biosci. Biotech. Bioch. 67:54–59.

Sun, C. Y., D. H. Li, Q. Liu, and B. H. Kong. 2014. Antioxidant activity and stability of maillard reaction products from whey protein derived peptide. Food Sci. 35:104–109.

Sun, Y. Y., D. D. Pan, and Y. X. Guo. 2010. Enzymatic hydrolysis of chicken protein and antioxidant activity of antioxidant peptide. Food Sci. 31:56–61.

Walter, J., Y. Greenberg, P. Sriramarao, and B. P. Ismail. 2016. Limited hydrolysis combined with controlled Maillard-induced glycation does not reduce immunoreactivity of soy protein for all sera tested. Food Chem. 213:742–752.

Wang, B., S. W. Zhang, L. Liu, X. Y. Feng, J. Lu, J. P. Lu, and J. H. Yu. 2018. Preparation and Emulsifying properties of maillard reaction products of sodium Caseinate. Food Sci. 39:98–104.

Xiong, G. Y., X. Gao, H. Zheng, X. Li, X. Xu, and G. Zhou. 2017. Comparison on the physico-chemical and nutritional qualities of normal and abnormal colored fresh chicken liver. Anim. Sci. J. 88:893–899.

Xiong, Q., M. H. Zhang, T. Wang, D. Y. Wang, C. Sun, H. Bian, P. P. Li, Y. Zou, and W. M. Xu. 2020. Lipid oxidation induced by heating in chicken meat and the relations with oxidants and antioxidant enzymes activities. Poult. Sci 99:1761–1767.

Yang, S. Y., S. W. Kim, Y. Kim, S. H. Lee, H. Jeon, and K. W. Lee. 2015. Optimization of Maillard reaction with ribose for enhancing anti-allergy effect of fish protein hydrolysates using response surface methodology. Food Chem. 176:420–425.

Zeng, Q. Z., Y. L. Cui, D. X. Su, T. Bin, S. He, and Y. Yuan. 2018. Process optimization and anti-oxidative activity of peanut meal Maillard reaction products. LWT - Food Sci. Technol. 97:573–580.

Zhang, H. C., J. Yang, and Y. Y. Zhao. 2015. High intensity ultrasound assisted heating to improve solubility, antioxidant and antibacterial properties of chitosan-fructose Maillard reaction products. LWT - Food Sci. Technol. 60:253–262.

Zou, T., L. Kang, C. Yang, H. Song, and Y. Liu. 2019a. Flavour precursor peptide from an enzymatic beef hydrolysate Maillard reaction-II: Mechanism of the synthesis of flavour compounds from a sulphur-containing peptide through a Maillard reaction. LWT - Food Sci. Technol. 110:8–18.

Zou, Y., H. Yang, P. P. Li, M. H. Zhang, X. X. Zhang, W. M. Xu, and D. Y. Wang. 2019b. Effect of different time of ultrasound treatment on physicochemical, thermal and antioxidant properties of chicken plasma protein. Poult. Sci 98:1925–1933.

Zou, Y., Y. Ding, W. Feng, W. Wang, Q. Li, Y. Chen, H. Wu, X. Wang, L. Yang, and X. Wu. 2016. Enzymolysis kinetics, thermodynamics and model of porcine cerebral protein with single-frequency countercurrent and pulsed ultrasound-assisted processing. Ultrason. Sonochem. 28:294–301.